Modelling Microtubules

1 Summary

Here we collect a short summary of the work done during this project. We began by building a bead-spring model of microtubules, consisting of single tubulins as beads and the bonds between them as springs. Each spring has a natural state, and deviations from this cause increased energy. This first included only spring length and spring bending. We then looked at single protofilaments, testing the efficiency of methods adding torsional energy into the bead-spring model, which in simple terms is the energy associated with twisting. Once torsion was added into our model, we looked at the different shapes of microtubules according to the number of constituent protofilaments and the helical rise.

With a working base model, further review of the literature led us to at least two phenomena we wanted to produce a model to explain. The first, delayed elongation and shrinkage in the presence and washing out of kinesin, indicated that (i) a conformational change was occurring which affected the longitudinal bonds and (ii) there is some memory which causes the delay. One interpretation of the memory is that there is a discrepancy between the local conformational changes and the global structure of the microtubule (i.e. a long microtubule is just very stiff), but another is that perhaps there is something slightly more complicated going on, with conformational states being somehwat separate to the kinesin presence. Tied up in this is also the fact that there seems to be evidence in [SMK+18] that there is a some sort of feedback loop between the presence of kinesin and a preference for kinesin bounding.

The second phenomena we wished to explain was the indication that there is a global bistability of the microtubule. This has been recorded in terms of the lateral spacing in the microtubule.

A possible mechanism through which both phenomena can be explained is in having a multiple state model. That is, each bead can change the characteristics of its bonds (stiffness, natural length, natural bend, etc) depending on the conformational state it is in. This introduces a kinesin-bound-like state. The switching between these conformational state is handled by introducing a transition rate which is based upon the energy that bead is experiencing. i.e. a bead in a high energy state will be likely to change

to a different conformational state. Kinesin bounding forces a particular conformational state, but the change can happen without the presence of kinesin. This can possible address all the phenomena we described above. Specifically:

- There can be a kinesin-bound-like conformational state which produces elongation.
- Tubulin in the kinesin-bound-like state may be more likely to have kinesin bound in the presence of kinesin.
- If kinesin is bound at a high density across the microtubule then when it is washed out each bead may not be in a very high energy state, meaning the switch back to the natural conformational state could be slow, producing the delays in shrinkage seen
- The kinesin-bound-like conformational state could affect the lateral bonds.
- For certain choices of kinesin-bound-like conformational states you may get a feedback effect, with neighbours being more likely to switch, producing persistence of clusters and bistability of the microtubule.

We now set out the model in more detail.

2 Model

2.1 One state model

In the same vein as other mesoscopic models of microtubules, we construct an energy function based on the displacements bond angles of the beads. We assume that the forces between adjacent tubulin monomers can be approximated by linear springs. In some recent studies nonlinear springs are used such as in [ZG20], we are mainly interested in the tensile and bending properties close to equilibrium whereas nonlinear springs are more appropriate in regions of large deformation.

Our model also hinges on the anisotropy of the tubulin monomers. As was discussed previously, bonds between tubulin are associated with specific sites and loops in the proteins. Hence, we encode this information as a single orientation Ω_i of each bead i. This orientation corresponds to a transformation from the global reference frame to the local reference frame. Traditionally, this transformation would be expressed as a rotation matrix calculated using Euler angles. In the reference frame of the bead the (usually four) bonds it makes with its neighbours have a natural or rest direction which we refer to by their roughly north, east, south, and west directions as observed from outside the microtubule: $\hat{\mathbf{v}}_i, i \in \{n, e, s, w\}$. Aside

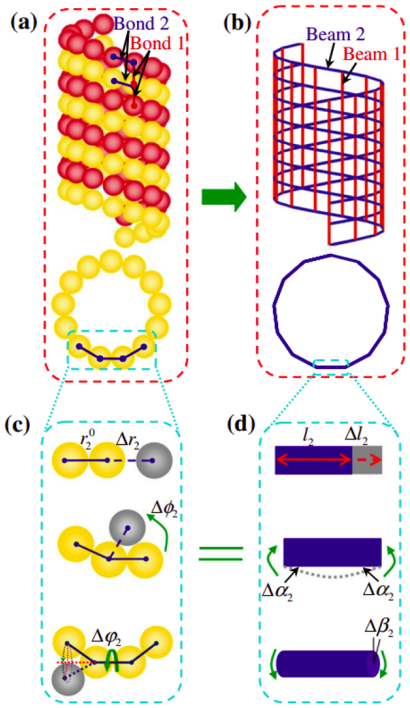

Figure 1: Above we see a figure taken from [ZW14], which summarises the model we start from here. Each tubulin is a bead, between which are bonds, each of which themselves have a natural length, bending angle, spring constant and bending stiffness. There is also a torsional energy.

from the linear forces from the linear springs then, there are also bending moments associated with the deviation of the bonds from their natural directions. Similarly, one could incorporate a torsional energy associated with the twisting of bonds from their natural directions.

We take the torsional energy exerted on a bead by its neighbour to be a function of the angle that the molecule would have to be rotated around the vector between them to be oriented in the same way in this frame of reference.

The total energy of the system is the sum of these components:

$$U = \sum_{i=1}^{N} \sum_{j \in \mathcal{A}_i} \left(U_{ij}^{\text{bond}} + U_{ij}^{\text{bend}} + U_{ij}^{\text{tors}} \right) \tag{1}$$

where $\mathcal{A}_i$ is the adjacency set for the bead i.

For each bond between two beads we have bead positions $\mathbf{x}_i$, $\mathbf{x}_j$ and relative displacement $\mathbf{r} = \mathbf{x}_j - \mathbf{x}_i$ (and we write $r = |\mathbf{r}|$). The beads have natural bond directions $\hat{\mathbf{v}}_i$, $\hat{\mathbf{v}}_j$ with bending angles $\theta_i = \cos^{-1}(\hat{\mathbf{r}} \cdot \hat{\mathbf{v}}_i)$, $\theta_j = \cos^{-1}(\hat{\mathbf{r}} \cdot \hat{\mathbf{v}}_j)$.

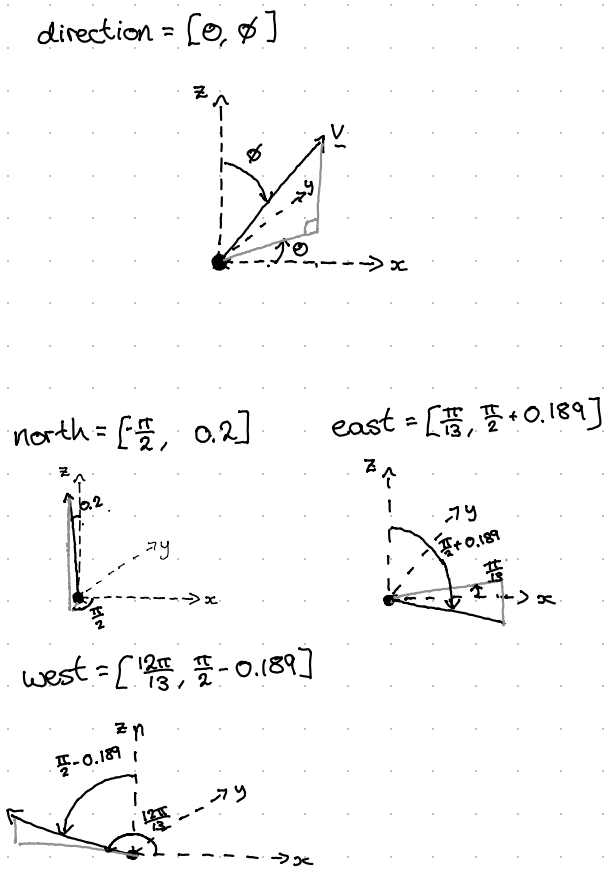

Figure 2: See above for an explanation of our angle-orientation convention. This is needed to convert angles into directions and vice versa.

The normal vector to the plane formed by the displacement and natural bond direction is denoted $\hat{\mathbf{n}}_i$ while the direction of increasing θ_i is written as $\hat{\boldsymbol{\theta}}_i$. The bond energy is simply a linear spring with natural length l_0 and spring constant k:

$$U_{ij}^{\text{bond}} = \frac{k_{ij}}{2}(r - l_0^{ij})^2. \tag{2}$$

The bending energy relates to the bending angle from the natural position. This could be a quadratic relationship, but it is perhaps easier to work with a cosine relationship because of its simple vectorial representation

$$U_{ij}^{\text{bend}} = K_{ij}[1 - (\hat{\mathbf{r}} \cdot \hat{\mathbf{v}}_i)] + K[1 - (\hat{\mathbf{r}} \cdot \hat{\mathbf{v}}_j)]. \tag{3}$$

The bending constants could be different on one side of the bond to the other but, in practice, they are the same for the time being.

The torsional energy relates to the rotation around the bond. Again, this can be a quadratic relationship but we work with a cosine relationship. Note that since, in practice, in a lattice these values are typically small, the quadratic relationship is well approximated by the cosine relationship.

$$U_{ij}^{\text{tors}} = K_{ij}^{\text{tors}}\left(1 - \left(\text{Proj}_{\hat{\mathbf{r}}}\left[\text{Orient}_i\left[\mathbf{w}\right]\right] \cdot \text{Proj}_{\hat{\mathbf{r}}}\left[\text{Orient}_j\left[\mathbf{w}\right]\right]\right)\right), \tag{4}$$

where $\text{Proj}_{\hat{\mathbf{r}}}$ is the projection to the plane defined by its normal $\hat{\mathbf{r}}$, and Orient_i is a function which takes a vector $\mathbf{w}$ and returns the vector corresponding to $\mathbf{w}$ in bead i's frame of reference. This is independent of the choice of the vector $\mathbf{w}$, so long as $\text{Orient}_i\left[\mathbf{w}\right]$ and $\text{Orient}_j\left[\mathbf{w}\right]$ are linearly independent to $\hat{\mathbf{r}}$. In practice this can be ensured by choosing a lateral bond direction when ij is a longitudinal bond, and a longitudinal bond when ij is a lateral bond.

Given the energy function, we find the forces and torques on the beads used to simulate the system by differentiating the energy with respect to the position and orientations. Firstly, the force is simply

$$\mathbf{F}_i = -\frac{\partial U}{\partial \mathbf{x}_i}. \tag{5}$$

The torque which alters the orientation of the bead can also be found from the potential energy. Writing $\hat{\mathbf{n}}_\chi$ as the axis of rotation for an angle $\chi_i \in \{\theta_i, \phi_i, \varphi_i\}$, we have

$$\boldsymbol{\tau}_i = -\sum_{\chi_i \in \{\theta_i, \phi_i, \varphi_i\}} \frac{\partial U}{\partial \chi_i} \hat{\mathbf{n}}_{\chi_i}. \tag{6}$$

In Appendix... details can be found of the calculations, but we just show the final results here. The total force on each bead is given by

$$\mathbf{F}_i = k(r - l_0)\hat{\mathbf{r}} + \frac{K_i}{r}\sin(\theta_i)\hat{\boldsymbol{\theta}}_{\boldsymbol{i}} - \frac{K_j}{r}\sin\left(\theta_j\right)\hat{\boldsymbol{\theta}}_{\boldsymbol{j}}. \tag{7}$$

The torque on the bead due to the bending energy is

$$\boldsymbol{\tau}_i = -K\sin(\theta_i)\hat{\mathbf{n}}_{\theta_i}. \tag{8}$$

2.2 Forces and torques

To find the forces acting on each bead, we use the derivative of the energy:

$$\mathbf{F}_a = -\frac{\partial U_{ij}}{\partial \mathbf{x}_a}, \quad a \in \{i, j\} \tag{9}$$

First, we find $\partial U_{ij} \big/ \partial \mathbf{r}$, from which the forces can easily be calculated using

$$\frac{\partial f}{\partial \mathbf{x}_i} = -\frac{\partial f}{\partial \mathbf{r}}, \quad \frac{\partial f}{\partial \mathbf{x}_j} = \frac{\partial f}{\partial \mathbf{r}} \tag{10}$$

for any scalar values function f. For the spring energy we have

$$\frac{\partial U_{ij}^{\text{bond}}}{\partial \mathbf{r}} = k_{ij}(r - l_0^{ij})\frac{\partial r}{\partial \mathbf{r}}. \tag{11}$$

It can be shown that $\partial r/\partial \mathbf{r} = \mathbf{r}/r$ and so the spring force is

$$\mathbf{F}_{ij}^{\text{bond}} = -\mathbf{F}_{ji}^{\text{bond}} = k_{ij}(r - l_0^{ij})\hat{\mathbf{r}}. \tag{12}$$

Leaving the bending energy in terms of the dot products enables us to find the force with relative ease. For the bending with respect to the bead a's natural direction $\hat{\mathbf{v}}_a$, we have

$$\begin{aligned}
\mathbf{F}_{ij}^{\text{bend}} &= \frac{\partial U_{ij}^{\text{bend}}}{\partial \mathbf{r}} && \text{(13a)}\\
&= K_{ij}\frac{\partial}{\partial \mathbf{r}}\left(1 - \frac{\hat{\mathbf{v}}_i \cdot \mathbf{r}}{r}\right) + K_{ij}\frac{\partial}{\partial \mathbf{r}}\left(1 - \frac{\hat{\mathbf{v}}_j \cdot \mathbf{r}}{r}\right) && \text{(13b)}\\
&= K_{ij}\left(\frac{\hat{\mathbf{v}}_i}{r} - \frac{\hat{\mathbf{v}}_i \cdot \mathbf{r}}{r^3}\mathbf{r}\right) + K_{ij}\left(\frac{\hat{\mathbf{v}}_j}{r} - \frac{\hat{\mathbf{v}}_j \cdot \mathbf{r}}{r^3}\mathbf{r}\right) && \text{(13c)}\\
&= \frac{K_{ij}}{r}\left[\hat{\mathbf{v}}_i - (\hat{\mathbf{v}}_i \cdot \hat{\mathbf{r}})\hat{\mathbf{r}}\right] + \frac{K_{ij}}{r}\left[\hat{\mathbf{v}}_j - (\hat{\mathbf{v}}_j \cdot \hat{\mathbf{r}})\hat{\mathbf{r}}\right] && \text{(13d)}
\end{aligned}$$

Now, this expression can be simplified greatly for computation by noticing that it is in the same direction as the direction of increasing angle, $\hat{\boldsymbol{\theta}}$. Specifically, for each bead $a \in \{i, j\}$:

$$\begin{aligned}
\hat{\boldsymbol{\theta}}_a &= \hat{\mathbf{r}} \times \hat{\mathbf{n}}_a = \hat{\mathbf{r}} \times \frac{\hat{\mathbf{v}}_a \times \hat{\mathbf{r}}}{|\hat{\mathbf{v}}_a \times \hat{\mathbf{r}}|} && \text{(14a)}\\
&= \frac{1}{\sin(\theta)}\left[(\hat{\mathbf{r}} \cdot \hat{\mathbf{r}})\hat{\mathbf{v}}_a - (\hat{\mathbf{r}} \cdot \hat{\mathbf{v}}_a)\hat{\mathbf{r}}\right] && \text{(14b)}\\
&= \frac{\hat{\mathbf{v}}_a - (\hat{\mathbf{r}} \cdot \hat{\mathbf{v}}_a)\hat{\mathbf{r}}}{\sin(\theta_a)} && \text{(14c)}
\end{aligned}$$

where we have used the triple vector product formula and used $|\hat{\mathbf{v}}_a \times \hat{\mathbf{r}}| = \sin(\theta_a)$. Substituting this into our expression for the bending force, we obtain

$$\mathbf{F}_{ij}^{\text{bend}} = \frac{K_{ij}}{r}\sin(\theta_i)\hat{\boldsymbol{\theta}}_{\boldsymbol{i}} - \frac{K_{ij}}{r}\sin\Big(\theta_j\Big)\hat{\boldsymbol{\theta}}_{\boldsymbol{j}}. \tag{15a}$$

Computationally it may make more sense to calculate the force in terms of eq. (13d) because the normalisation and sine computations do not need to be carried out.

The torque which alters the orientation of the bead can also be found from the potential energy. Writing $\hat{\mathbf{n}}_\chi$ as the axis of rotation for an angle $\chi \in \{\theta, \phi, \varphi\}$, we have

$$\tau_\chi = -\frac{\partial U_{ij}}{\partial \chi}\hat{\mathbf{n}}_\chi. \tag{16}$$

Now, for the bending potential, we know $U_{ij}^{\text{bend}} = K_{ij}[1 - \cos(\theta_i)] - K_{ij}[1 - \cos\Big(\theta_j\Big)]$. So taking the axes to be such that the planes line-up, we find

$$\tau = \sum_\chi \tau_\chi = -\frac{\partial U_{ij}}{\partial \theta_i}\hat{\mathbf{n}}_{\theta_i}. \tag{17}$$

$$= -K_{ij}\sin(\theta_i)\hat{\mathbf{n}}_{\theta_i} \tag{18}$$

2.3 Over-damped equations of motion

To integrate in time, we assumed the system is over-damped. That is, the linear and angular momenta (and hence linear and angular velocities $\mathbf{v}, \boldsymbol{\omega}$) decay sufficiently quickly that they are proportional to the force and torque, respectively. Writing γ_θ as the rotational friction coefficient, we use

$$\boldsymbol{\omega}(t) = \frac{1}{\gamma_\theta}\boldsymbol{\tau}(t), \tag{19}$$

$$\mathbf{v}(t) = \frac{1}{\gamma_x}\mathbf{F}(t), \tag{20}$$

In terms of quaternions, Euler's equations of motion for a rotating body is given by

$$\dot{q} = \frac{1}{2}\tilde{\omega}(t) \cdot q(t) \tag{21}$$

where $q(t)$ is the orientation of the body and $\tilde{\omega}(t) = [0, \boldsymbol{\omega}(t)]$. Using our over-damped assumption, this becomes

$$\dot{q} = \frac{1}{2\gamma_\theta}\tilde{\tau}(t) \cdot q(t) \tag{22}$$

with $\tilde{\tau} = [0, \boldsymbol{\tau}] \coloneqq 0 + \tau_x \mathbf{i} + \tau_y \mathbf{j} + \tau_z \mathbf{k}$. Hence, the orientation is updated according to

$$q_i(t + \Delta t) \approx q_b(t) + \frac{\Delta t}{2\gamma_\theta} \tilde{\tau}_i(t) \cdot q_i(t), \tag{23}$$

with $\tilde{\tau} = [0, \boldsymbol{\tau}]$. The position is then updated according to

$$\mathbf{x}_i(t + \Delta t) \approx \mathbf{x}_i(t) + \frac{\Delta t}{\gamma_x} \mathbf{F}_i(t). \tag{24}$$

If fluctuations need to be considered, we can use the Euler-Maruyama scheme.

2.4 Comments on the model

Our spring and bead representation of the bonds in a microtubule is, of course, a simplification. For one, the contact surface between two adjacent tubulin is far more complex than just a one dimensional spring connecting the two centres. Indeed, in the real life case it is even unclear what a distance between tubulin really means. Some parts of the tubulin are touching and some aren't.

We take a linear elasticity simplification here. This is accurate for small changes in state, but Hooke's law fails to accurately model the dynamics of springs acting non-linearly, for example in the case of large deformations. So long as we initialise our dynamics sufficiently close to equilibrium, this should not pose significant issues.

There is a substantial amount of parameters here. It is difficult to find reasonable values for the stiffness and equilibrium of each type of bond. We have done this by taking values found from molecular dynamics simulations of microtubules in the literature. These should not be taken without scrutiny.

2.5 Two/three state model

From here, we wish to develop a model which can describe some of the phenomena observed when Kinesin is attached.

We model the kinesin attachment in the following way. When Kinesin attaches to a dimer, it affects the natural equilibrium. i.e. it can change K_{ij}, k_{ij}, l_0^{ij}, etc. In this way we need to introduce a variable $s \in \{-1, +1\}$ for each tubulin which describes the state so that we have the parameters K_{ij}^s, k_{ij}^s, $l_0^{ij;s}$, where s is -1 in the natural state and is 1 when kinesin is attached or if kinesin is unattached but it is in the kinesin like state.

There are several possible conformational changes.

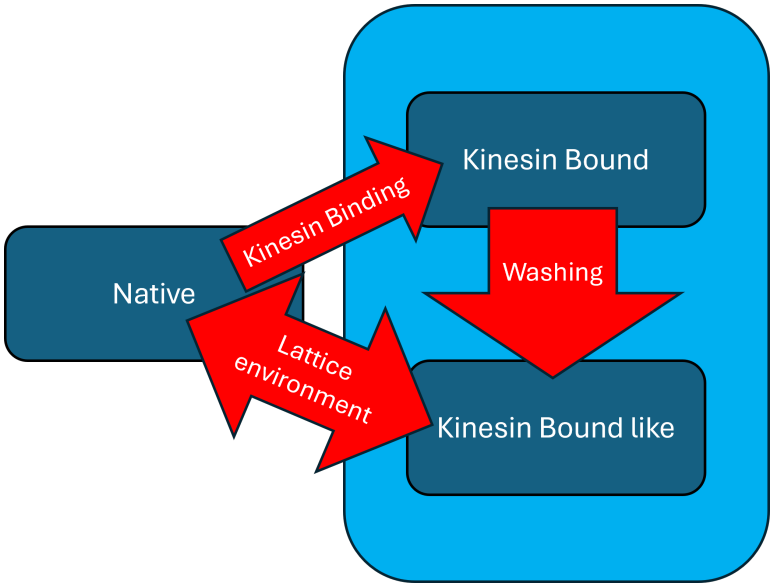

Figure 3: This diagram shows the introduction of the multiple state model. While there are two conformational states (i.e. two sets of corresponding parameters) the second conformational state is split into two further states – one in which it cannot jump out of, and one it can. This represents the kinesin bound state and the kinesin bound like state.

We use Kramer's theory of reactions to model the changes between conformational state. More concretely, if the total energy of a tubulin in state $s \in \{-1, +1\}$ is U_s, then the rate of switching to state $-s$ is

$$A_s e^{-U_s/k_B T}. \tag{25}$$

We note that this is equivalent to each state having an intrinsic energy attached, since

$$A_s e^{U_s/k_B T} = e^{U_s/k_B T + \log(A_s)} = e^{\frac{(U_s + k_B T \log(A_s))}{k_B T}} = e^{\frac{U_s + \bar{U}_s^0}{k_B T}} \tag{26}$$

where $\bar{U}_s^0$ is the energy of being in the state s, independent of the local environment.

Simply, if the energy that a tubulin experiences is high, then it will be more likely to change state.

2.6 Conformational states

Here we define four different candidate conformational changes which could explain certain data in the literature.

2.6.1 Longitudinal extension - There are two possible conformational changes which could explain longitudinal These two can be seen in Figure 10. In both cases, this can either lead to elongation of the whole microtubule (as in the case where there are equal amounts of tubulin in kinesin-bound-like state around the circumference of the tube) or bending (in the case where one of the constituent protofilaments has more tubulin in the kinesin-bound-like state than the rest).

1. One option is for the natural length l_0 of the spring bond to be increased for beads in the kinesin-bound-like state. This simply means that each constituent protofilament would be extended and therefore the microtubule would be extended.

2. Another option is for the natural state to, instead, be such that the alpha and beta tubulin have a mismatch in the stiffness of the spring bend. This means that, rather that straight, the natural state would be zig-zagged. Then, if in the kinesin-bound-like state both alpha and beta had the same stiffness, the bond would be forced to be straight.

2.6.2 Lateral crinkling - We propose two possible conformational changes which could explain the lateral crinkling in [DCL+20].

1. One could have that the bend angle is increased. In this sense you would have higher curvature areas and lower curvature areas, producing some form of crinkling.

2. Perhaps more simply, it might be that the natural length of the lateral spring is increased for the second conformational state.

2.7 Parameters

In Table 1 we can see the parameter values, mostly taken from [ZW14]. While these parameters are fairly widespread throughout the literature, we did identify that they all come from one paper which obtained them through molecular dynamics. This may not be ideal.

3 Comparison with literature

Here we write some words about two main papers about which we discuss. First, we discuss Shima. This paper is a trove of experimental data, but can be difficult to parse because of all the different moving parts. One thing that they show in [SMK+18] is a delay in the elongation and relaxation of the microtubule . This leads us to believe there is some sort of memory in the microtubule. We should say that this is still up for debate and there is not consensus in the literature about this point. We can obtain this delay

Parameter	Units	Value	Source
K_{lat}	$\text{nN} \cdot \text{nm/rad}^2$	8.5	[ZW14]
K_{in}	$\text{nN} \cdot \text{nm/rad}^2$	2	[ZW14]
K_{long}	$\text{nN} \cdot \text{nm/rad}^2$	2	[ZW14]
k_{lat}	N m^{-1}	14	[ZW14]
k_{in}	N m^{-1}	3	[ZW14]
k_{long}	N m^{-1}	3	[ZW14]
l_0^{lat}	nm	5.16	[ZW14]
l_0^{in}	nm	4.05	[ZW14]
l_0^{long}	nm	4.05	[ZW14]
η	$\text{Pa} \cdot \text{s}$	0.2	[KKK$^+$22]
R_{bead}	nm	2	[KKK$^+$22]
a	nm	4.05	[JF11]
δx	nm	5.13	[JF11]

Table 1: Parameter values used in simulations and their source. The natural bond directions will also need to be specified as well as the drag coefficients.

in elongation and relaxation with our conformational states – simply slow enough transition rates mean that this is achieved.

Now, [DCL$^+$20]. In [DCL$^+$20] they study potential conformational changes of the microtubule, specifically with respect to the lateral bonds. They record the distribution over the angle between neighbouring tubulin, and find that this can sometimes exhibit bimodality. They describe this as crinkling, which suggests a 'crinkle' of the wall of the microtubule, with some tubulin sticking out. That is, if one was to project the tube wall down onto a 2D plane, one would see zig-zagging rather than a circle. However, this is not the only interpretation of their results. A bimodal distribution could also be seen if, say, the circle was actually an ellipse. One can do a quick analytic calculation for this, which we record below. If one ignores longitudinal bonds, and simplifies to a 2D problem, then for a chain of N tubulin to connect back up while under no lateral bend angle stress, one needs

$$N_{flat}\theta_{flat} + N_{tight}\theta_{tight} = 2\pi,$$

where θ_{flat} and θ_{tight} are the natural bending angles of the tubulin in the

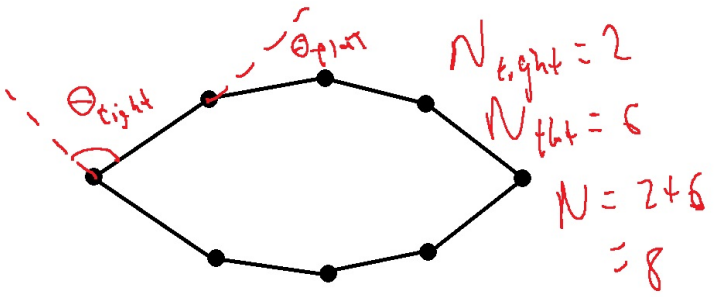

Figure 4: Here we see the ellipse interpretation of the results in [DCL+20]. This would exhibit bimodality in the angle.

different conformational states.

In our model, we can start in . This is also highly dependent on the boundary conditions. It is not clear what the right fixing of the bottom ring should be. In these cases it is probably best to fix the orientation of the bottom bead and have a free boundary condition.

4 Open questions

There are numerous issues with the model as is, some of which we were able to address throughout this project. Here we list them

- Speed of simulation. At the moment, we can simulate microtubules roughly the length of 120 dimers for time on the order of *ms*. This is roughly $0.5\mu m$. This is still not the length of microtubules experiments are done with, and certainly not the timescales apparent in the dynamics of microtubules. There are a number of things can could be done to mitigate this, the first and most obvious being to parallelise the code. In a long microtubule not all parts will affect eachother so one could consider different patches independently then stitch them together.

- Boundary conditions: for some experiements, microtubules must be fixed at the bottom. For others, both ends must be fixed. Sometimes, one wishes to have both ends free. In our simulations, we can do each of these, but they introduce some instabilities and erroneous dependencies. We found that the fixing of one end (the entire lowest ring) affects quite far up the microtubule. To simulate free ends, one can fix the orientation of one bead. In this case one can simply think of the frame of reference changing. Another possibility is to simulate an infinitely long, periodic microtubule. Here there is some complication

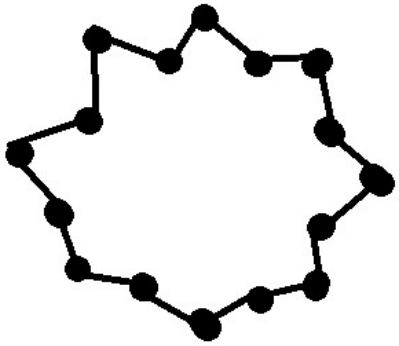

Figure 5: Here we see the true 'crinkling' interpretation of the results in [DCL+20]. This would also exhibit bimodality in the angle. More specifically, here we have two different natural bend angles of bonds. if there are two with a larger natural bend angle (in the case of above where there are 8 in total, with 6 having a smaller natural bend angle), then it is energetically favourable for the structure to be arrange as above.

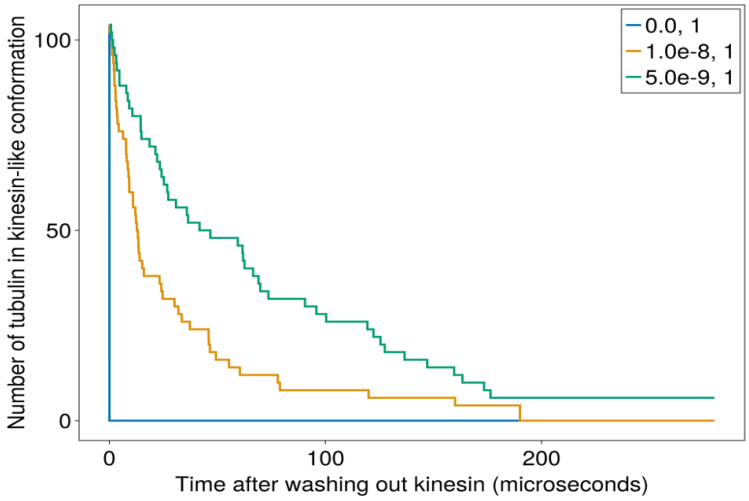

Figure 6: Above we see that by changing the transition rate A_s, one can alter the decay of the clusters of kinesin-bound-like tubulin. By delaying this decay, one also necessarily has that the shrinkage of the microtubule would be delayed, as observed in [SMK+18] (see Figure 8).

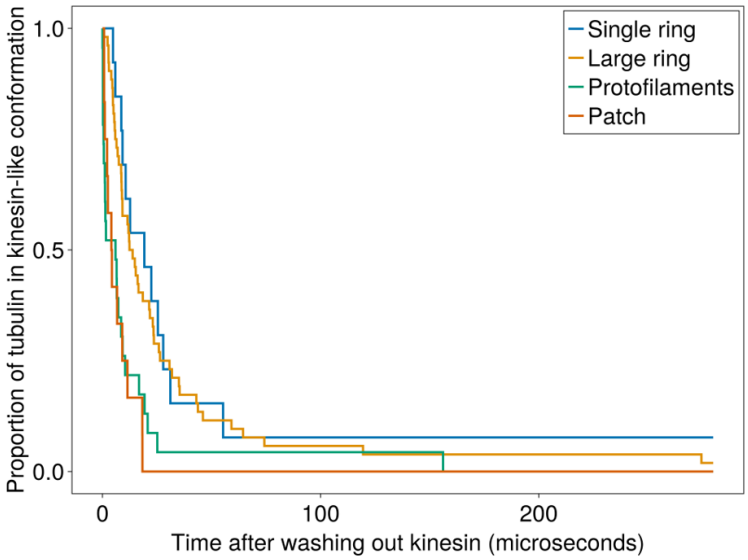

Figure 7: Here we see that the shape of the original kinesin-like cluster affects the time that it takes to decay. We test 4 different shapes. For the single ring we bound kinesin on a ring of tubulin. For the large ring we bound a block of 4 rings. For protofilaments we bound a whole single protofilament. For patch it is a 3 by 3 square of tubulin.

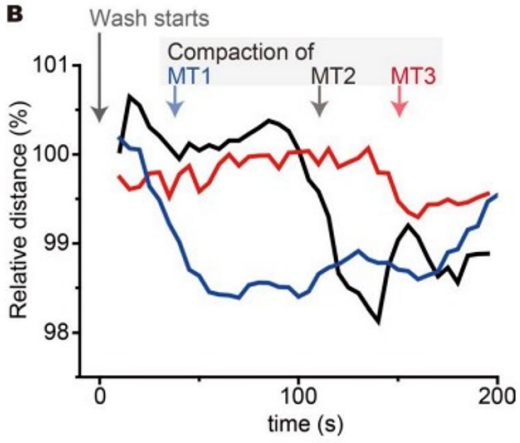

Figure 8: Above we see a figure taken from the supplementary material of [SMK+18], which shows the delay in the contraction of the microtubule back to natural size. It indicates that there is, perhaps, some memory within the microtubule. This is one phenomena our two/three state model aims to address. See Figure 9 for such extended contraction with our three state model.

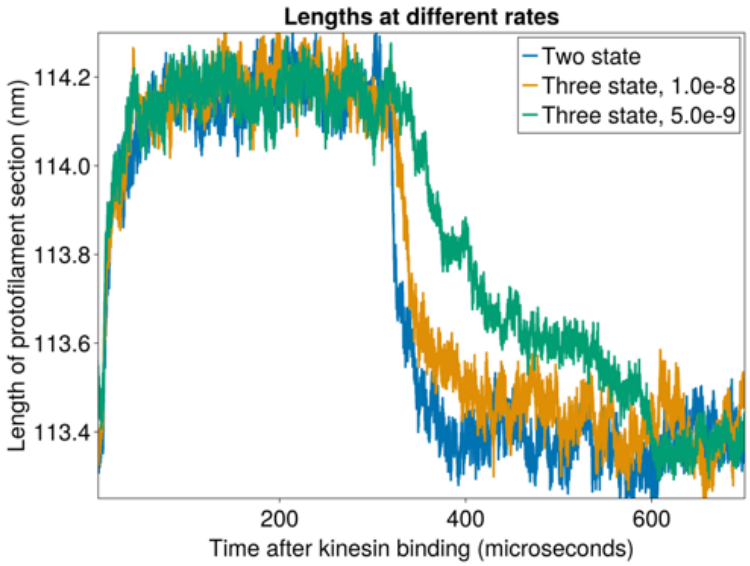

Figure 9: Above we see the delay of the contraction of the microtubule. We take a microtubule, bind kinesin to every tubulin, and then at $300\mu s$, we imediately wash off all kinesin. Note that in the three state model, this does not mean the tubulin immediately go back to the natural conformational state. Hence, we get some delay in the length. See also Figure 6 for what this means in terms of the number of kinesin-bound-like tubulin.

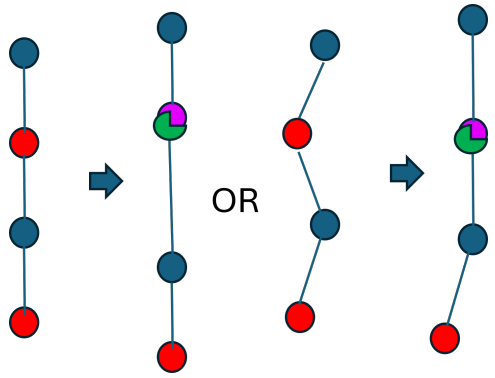

Figure 10: Here we see the two possible types of elongation of a protofilament that we propose in this report. On the left hand side, we have simply extension of the natural spring length. On the right hand side, we have a stiffening or straightening of the protofilament, causing it to move from being zig-zagged to straight.

because it is not clear how to 'stitch' together the sections. This is something to think about in the future.

- There are clearly multiple timescales when it comes to the microtubules. Locally, the beads seem to relax very quickly, on the order of μs or even ns, see for example Figure 9
- At the moment it is not clear that we gain anything 'extra' by adding these extra conformational states. Our model can now, of course, exhibit multiple states and this can lead to the elongation of the microtubule, as seen in Figure 10. However, what we are yet to see is coexistence and true bimodality.

5 Conclusion

It is difficult to make concrete conclusions from the work done with this project. It is a long-term vision to describe, at a meso level, the dynamics of a microtubule. We have introduced a new element into our model which has not been seen in the literature – that of the different conformational states and environmentally dependent switching between them. This change goes some way to explaining some of the phenomena, but still needs to be explored. The code for this model is uploaded on github and from there perhaps more developments can be made to produce a model which truly does explain the phenomena observed and can reliably inform experimentalists as well as be informed by experimental data.

References

[DCL+20] Garrett E. Debs, Michael Cha, Xueqi Liu, Andrew R. Huehn, and Charles V. Sindelar. Dynamic and asymmetric fluctuations in the microtubule wall captured by high-resolution cryoelectron microscopy. *Proceedings of the National Academy of Sciences*, 117(29):16976–16984, 2020.

[JF11] Xiang-Ying Ji and Xi-Qiao Feng. Coarse-grained mechanochemical model for simulating the dynamic behavior of microtubules. *Physical Review E*, 84(3):031933, September 2011. Publisher: American Physical Society.

[KKK+22] Evgenii Kliuchnikov, Eugene Klyshko, Maria S. Kelly, Artem Zhmurov, Ruxandra I. Dima, Kenneth A. Marx, and Valeri Barsegov. Microtubule assembly and disassembly dynamics model: Exploring dynamic instability and identifying features of Microtubules'

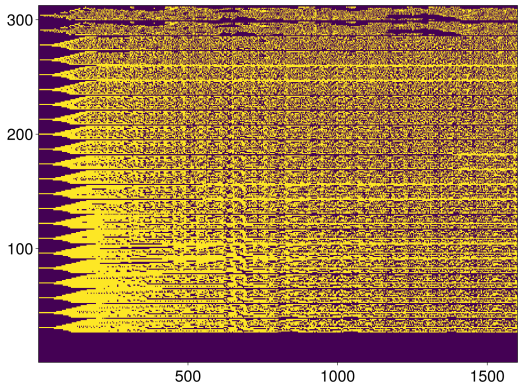

(a)

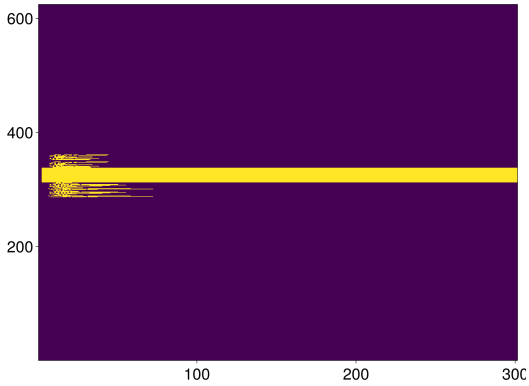

(b)

Figure 11: In this plot we have listed all tubulin in a microtubule (y axis) across time, showing which conformational state it is in. The middle band in the botton is in a forced kinesin like state, while in the top there is no forced kinesin like state. Here we see the two types of behaviour we get at the moment. There is either completely random switching of conformational state or you get a big burst at the beginning followed by it dying out very quickly. We think this may be because of the inherent difference in the timescales. The conformational switching is happening on a local time scale which is much faster (since it is about the strain of individual beads) than the relaxation of the microtubule. Hence, we get massive increases of clusters at the beginning but they cannot hope to persist. One can hugely reduce the transition rates, of course, but this leads to no increase of clusters at all.

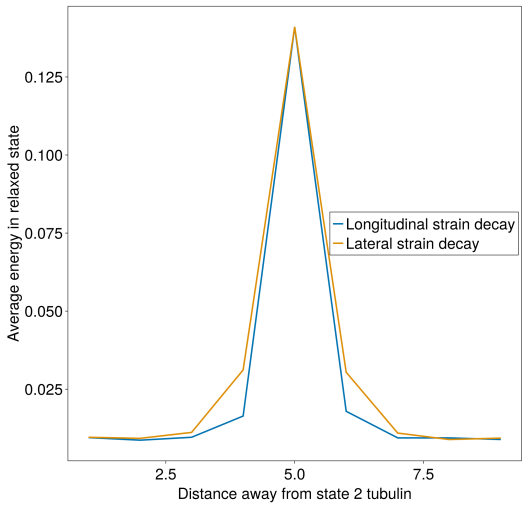

Figure 12: Above we see, in the case of the changing of the stiffness (i.e. 2 in the longitudinal extension candidates), how the strain is distributed across the neighbouring tubulin. We see there is a very quick drop off in strain, meaning the local. This has consequences for our two/three state model, since it means the neighbours are not under anywhere near as much strain as the kinesin-bound-like tubulin itself. This, in turn, means that it will be likely to switch back to natural state before influencing any of its neighbours to switch. Hence the only way one can get real prevalence of clustering across a microtubule would be to have lots of forced kinesin bound tubulin which could not switch back. The y-axis here is in $0.01k_BT$

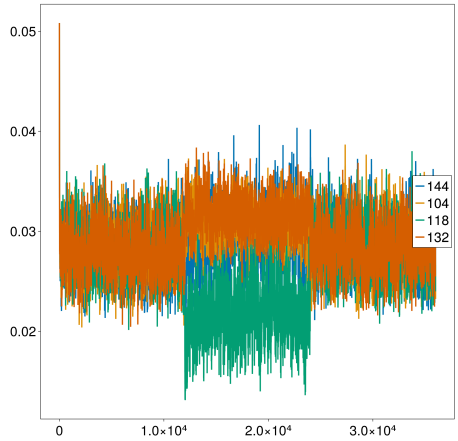

Figure 13: This plot shows that when the microtubule is in a relatively high-energy state some peculiar things can happen. Here, specifically, we plot the energy of a tubulin which we force to be kinesin bound and its longitudinal neighbours (which we don't). We see that the tubulin below is actually is a less-strained state than before. This is because of the off-set angle which dictates that tubulin bonds want to be slightly bent. Here the x-axis is time in μs and the y-axis is energy ($0.005 k_B T$)

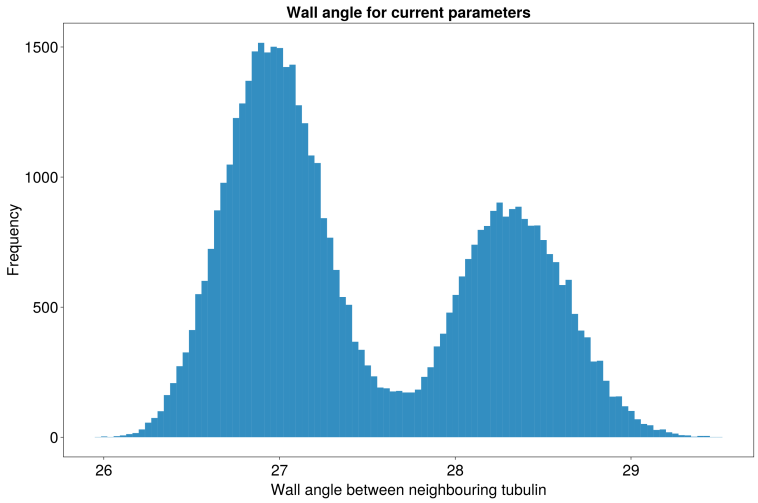

Figure 14: Above we see that we can recreate a bimodal distribution, but note that we were not able to do this with the three state model. This is using the first of the possible candidates for conformational states discussed before. Specifically, this is the mechanism in which a kinesin-bound tubulin has a larger natural bend angle than the normal state. One can see that the differences in the peaks are still too small in comparison with that in [DCL+20]

Growth, Catastrophe, Shortening, and Rescue. *Computational and Structural Biotechnology Journal*, 20:953–974, January 2022.

[SMK+18] Tomohiro Shima, Manatsu Morikawa, Junichi Kaneshiro, Taketoshi Kambara, Shinji Kamimura, Toshiki Yagi, Hiroyuki Iwamoto, Sotaro Uemura, Hideki Shigematsu, Mikako Shirouzu, Taro Ichimura, Tomonobu M. Watanabe, Ryo Nitta, Yasushi Okada, and Nobutaka Hirokawa. Kinesin-binding–triggered conformation switching of microtubules contributes to polarized transport. *Journal of Cell Biology*, 217(12):4164–4183, 10 2018.

[ZG20] Jin Zhang and Siwen Guan. Tensile properties of microtubules: A study by nonlinear molecular structural mechanics modelling. *Physics Letters A*, 384(27):126674, September 2020.

[ZW14] Jin Zhang and Chengyuan Wang. Molecular structural mechanics model for the mechanical properties of microtubules. *Biomechanics and Modeling in Mechanobiology*, 13(6):1175–1184, November 2014.